Available online at www.sciencedirect.com
SCIENCE DIRECT
Polymer 46 (2005) 12359–12365
polymer
www.elsevier.com/locate/polymer

Universal yield stress function for biocompatible chitosan based-electrorheological fluid: Effect of particle concentration

Jun Hee Sung [a], Won Hyu Jang [a], Hyoung Jin Choi [a,*], Myung S. Jhon [b]

[a] Department of Polymer Science and Engineering, Inha University, Incheon 402-751, South Korea
[b] Department of Chemical Engineering, Carnegie Mellon University, Pittsburgh, PA 15213, USA

Received 28 March 2005; received in revised form 19 October 2005; accepted 28 October 2005
Available online 14 November 2005

Abstract

Electrorheological (ER) response of biocompatible particles suspended in an insulating silicone oil, was investigated under several different applied external electric field strengths. Chitosan, a biodegradable polysaccharide, was used as anhydrous ER materials. The effect of particle volume concentration on their ER response was examined by focusing on the measurement for rheological and electrical properties. The yield stress of chitosan suspended in silicone oil system as a function of applied electric field strength showed different value of slopes for different particle concentrations, however, all data points collapse onto a universal scaling function.

Keywords: Electrorheological fluid; Chitosan; Yield stress

1. Introduction

Electrorheological (ER) fluid, typically a suspension of semiconducting or dielectric solid particles in electrically non-conducting liquid media, exhibits rapid and reversible change in shear viscosity under the imposed electric field. This phenomenon originates from the aggregation of the solid particles due to attractive forces, induced by the external field [1–5], among the dipolar moments. The reversible behavior on the order of millisecond is related to dielectric properties including interfacial polarization. The migration of mobile charges is caused by the increase in polarizability of the particle and results in a larger dipole moment. These field induced dipoles attract each other and cause the particles to form chains or fibrillar structures in the direction of the electric field. These chains are formed by interparticle forces which exhibits sufficient strength to inhibit fluid flow, i.e. these colloidal suspensions with high electric field strength and particle concentration, exhibit strong resistance against a shear deformation. The most significant change in the material characteristics for ER fluids is associated with the yield stress, which depends on the applied electric field strengths. Anhydrous ER materials are polarizable with conducting and electroluminescent material, including polyaniline and its derivative [6–8], inorganic particles with a polyaniline coating [9,10], polythiophene [11], poly(acenequinone) radicals [12], poly(*p*-phenylene) [13], and polymer/clay nanocomposites [14–16]. Recently, biopolymers, as a new anhydrous material, have been used to prepare ER fluid systems. These include phosphate cellulose and chitosan derivatives, such as chitosan adipicate suspension [17], chitosan sulfate suspension [18], and dihydroxylpropyl chitosan suspension [19].

These imply that synthetic conducting polymers and polymers with branched polar groups such as amino ($-NH_2$), hydroxy (–OH), and amino-cyan (–NHCN) can be used as the disperse phase of the ER suspension [20,21]. The polar groups affect the ER response by playing the role of an electronic donor, therefore the chemical structure of the organic materials becomes an important factor in determining the ER properties. Since the chemical natures including molecular and crystal structures determine the dielectric and polarization properties, it is possible to modify the dielectric and polarization properties to increase ER effect.

The chitin, among various natural polymers, is a macromolecule which consists of 2-acetamide-2-deoxy-β-D-glucose through the β-(1-4)-glycoside linkage, which is widely spread in the shells of crabs, lobsters, shrimps, and insects. The principal derivative of chitin is a chitosan, which is a linear polysaccharide of poly[β-(1→4)-2-amino-2-deoxy-D-glucopyranose]. As the degree of deacetylation of chitinous material

* Corresponding author. Tel.: +82 32 860 7486; fax: +82 32 865 5178.
E-mail address: hjchoi@inha.ac.kr (H.J. Choi).

0032-3861/$ - see front matter © 2005 Elsevier Ltd. All rights reserved.
doi:10.1016/j.polymer.2005.10.133

exceeds 50%, it becomes soluble in acidic aqueous solutions. The difference between chitin and chitosan is their capability to solubilize in dilute acidic media. This is produced by alkaline deacetylation of chitin by removing acetyl groups from *N*-acetyl glucosamine residues, leaving exposed amine groups capable of attaining positive charges in aqueous solutions at low pH. This active amine group provides several unique chemical and physical properties to the chitosan polymer. Both crystallizable [22] chitosan and chitin with excellent mechanical properties are very attractive materials particularly in pharmaceutical applications [23,24] since they can also be used as drug carriers.

In this study, we adopted chitosan particles as anhydrous particles in dry-base systems as a continuation of our previous study [25]. The chitosan particles based ER fluids were examined via electrical properties, dielectric characteristics, as well as rheological properties, including yield stress. We correlated the critical yield stresses with the polarization and conduction models for the chitosan-based anhydrous ER system, mainly by focusing on dispersed particle concentrations.

2. Experimental

Chitosan, widely distributed in nature [26], is a series of different deacetylated (higher than 50%) chitin derivatives. It is classified as a cationic polyelectrolyte since only the amino polysaccharide of which the amino group in the backbone of the molecule can be easily protonated in acidic solutions. Schematic diagram of the chemical reaction producing chitotan from chitin is as follows:

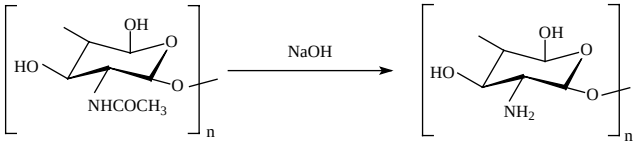

The chitosan, used as an anhydrous ER material, is a commercial powder supplied by Samchully Pharm. (Korea), which is 95% deacetylated. To remove any trace of moisture for the application of anhydrous ER systems, chitosan particles were placed in a vacuum oven for two days at room temperature prior to use. ER fluids were then prepared by dispersing appropriate amounts of chitosan particles in silicone oil (viscosity: 50 cS). The chitosan based ER fluids with three different volume fractions (22, 29, and 37 vol%) were prepared. The density of the chitosan and silicone oil was 0.68 and 0.96 g/ml at 25 °C, respectively.

Electrical conductivity of the chitosan particles was measured to be 5.26×10^{-10} S/cm using a two-probe method with the 13 mm pellet type KBr. Rheological properties of the chitosan-based ER fluids with and without an applied electric field were examined using a rotational rheometer (Physica MC120, Stuttgart, Germany) with a Couette geometry (Z3-DIN) equipped with a high-voltage generator (HVG 5000, Stuttgart, Germany). Temperature was controlled via circulating oil bath (Viscotherm VT 100). Several Dc electric field strengths (0.5–2.5 kV/mm) were applied to the insulating bob. The flow curves were measured via the controlled shear rate (CSR) mode in which the shear rate was applied to the ER fluid and the resulting shear stress was measured [27]. The ER fluid (in a controlled shear stress (CSS) mode) was also stressed by an applied mechanical torque until the particle chain was broken to initiate flow. The shear stress at an onset of the flow with CSS mode was reported as a static yield stress. This yield stress is strongly dependent on the electric field strength and increases with particle concentration [28]. Furthermore, the dielectric relaxation spectra of all prepared ER fluids were examined using the HP 4282A Precision LCR meter with HP 16452A liquid test fixture. Frequency of AC electric fields ranged from 20 Hz to 1 MHz. All these experiments were performed at 25 °C.

3. Results and discussion

Fig. 1 shows scanning electron microscope (SEM) photograph of the chitosan particles. The particle shape was observed to be irregular with rough surface in which the particle size of the chitosan was adjusted by using a 100 μm sieve prior to the ER measurement.

Fig. 2 shows the Fourier transform infrared spectroscopy (FT-IR) spectrum of the chitosan particles. The peaks observed the OH and NH_2 at 3000–4000 cm^{-1}, the C=O of $NHCOCH_3$ which indicates small amount of remaining chitin at 1663 cm^{-1}, the C–H stretching at 2878 cm^{-1}, and the C–H bending at 1376 cm^{-1}, respectively. In addition, the characteristic peaks shows the C–O–C at 1077 cm^{-1} and amide (O=CN) at 1423 cm^{-1}.

Fig. 3 shows flow curves for the chitosan based ER fluids in silicone oil (29 vol% of particle concentration) at six different electric field strengths obtained from the CSR mode. The fluid behaves like Newtonian in the absence of an applied electric field representing a slope of 1.0. When the electric field is applied the shear stress (for all shear rates) of ER fluid increases with the electric field strength since interparticular interactions enhance the shear stress as the particle formed the fibrillar structures. This behavior is described by the following

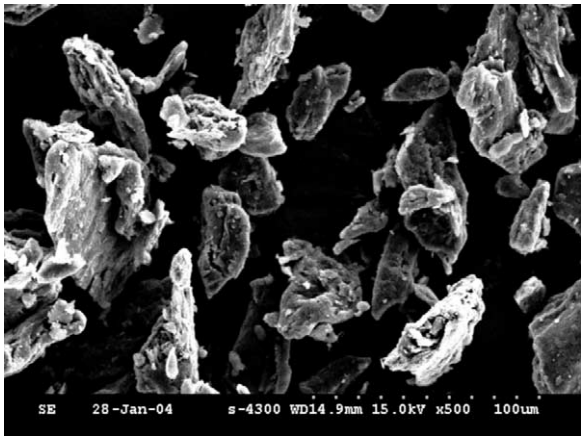

Fig. 1. SEM photograph of chitosan particles.

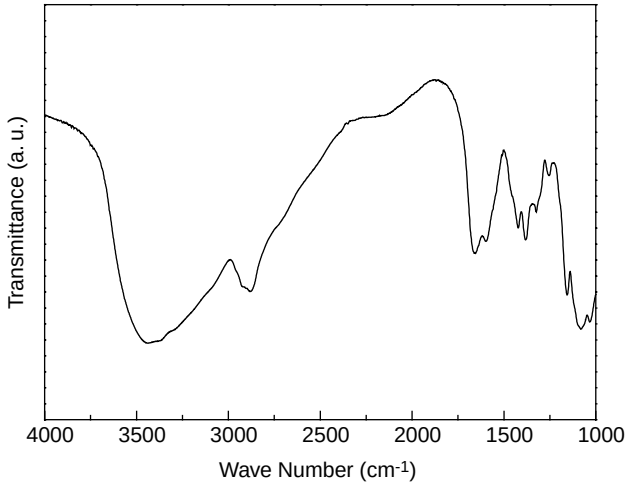

Fig. 2. FT-IR spectrum of chitosan particles.

Bingham fluid model in general,

$$\tau = \tau_y + \eta\dot{\gamma} \quad \tau \geq \tau_y$$
$$\dot{\gamma} = 0 \quad \tau \leq \tau_y \tag{1}$$

Here, τ_y is the yield stress and is a function of an electric field strength, τ is the shear stress, $\dot{\gamma}$ is the shear rate, and η is the shear viscosity. The yield stress, the critical parameter in ER response, depends on the electrical field strength and particle volume fraction.

As we increase the shear rate, the fibrillar structure of particles aligned in the applied electric field direction is distorted and destroyed via an imposed strain. However, the shear stress remained approximately constant (plateau region) as the shear rate increased up to a certain critical value, where the electrostatic force becomes approximately enough to the hydrodynamic force as shown in Fig. 3. This flow behavior at a plateau region can be compared with other ER fluids showing a critical shear rate, which corresponds to a transition point to the Newtonian-fluid region after decrease in the shear stress.

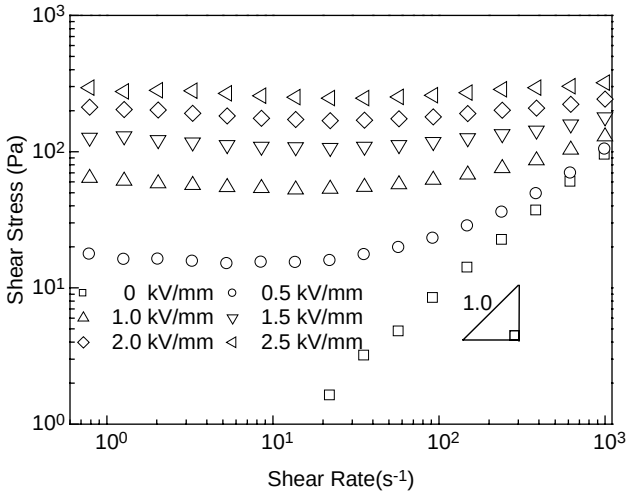

Fig. 3. Shear stress vs. shear rate for 29 vol% chitosan particle suspended in silicone oil for six different electric field strengths.

At a low shear rate region, the electrostatic interactions among particles (induced by the applied electric fields) are dominant compared to the hydrodynamic interactions (induced by the external flow field). The aligned particular structures begin to break with shear deformation, and these broken structures tend to reform chains by the applied electric field, depending on the applied shear strength and particle–particle interaction in the fibrils [29]. In the presence of an applied electric field, the Mason number, which is the ratio between the viscous forces which tend to disrupt the structure and the polarization forces responsible for the structural formation, has been used to quantity the interplay between dipole force and flow [30].

The shear stresses of the ER fluid at specific shear rates ($\dot{\gamma} = 10$ and 100 s^{-1} in Fig. 3) are shown in Fig. 4 as a function of the applied electric field strength. The slope in Fig. 4 shows the deviation from the polarization model, $\tau \propto E^2$ [31]. The polarization model is obtained from the attractive force between particles like Maxwell–Wagner's interfacial polarization and applied point-dipole approximation [32]. The slopes we obtained are 1.75 ± 0.02 at $\dot{\gamma} = 10\ s^{-1}$ and 1.50 ± 0.01 at $\dot{\gamma} = 100\ s^{-1}$. These differences of the slope at the given shear rates indicate the relation between interparticle electrostatic force and hydrodynamic force. It also demonstrates that the exponent deviates from two (expected from the polarization model) under the shear (nonzero $\dot{\gamma}$). This slope change also indicates that the flow field with a hydrodynamic force induces less dependence of the applied electric strength as the shear rate increases and finally in the high shear rate region, all the flow curves merge to that with zero applied electric field strength.

Fig. 5 presents the dependence of static yield stress (τ_y) on electric field strength of suspended chitosan in silicone oil for different volume fraction from the CSS mode. The yield stress originates from the attractive forces between particles, by fully taking into account both polarization and conduction models. The nonlinear conductivity effect with the bulk conducting particle model and the exponent of the power law is 1.5 at high electric field strengths.

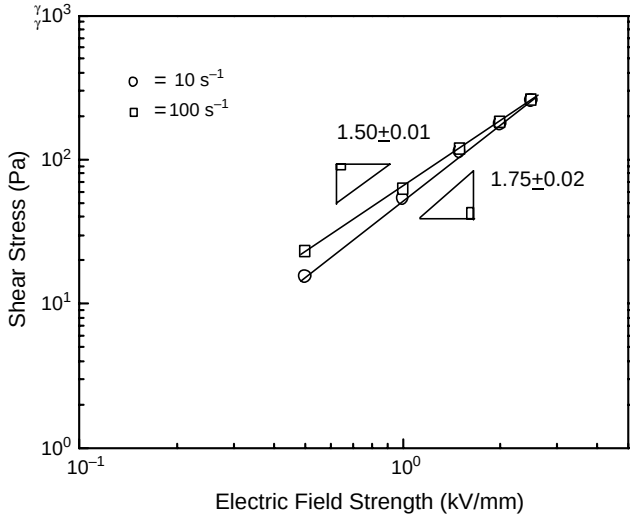

Fig. 4. Shear stress vs. electric field strength for chitosan particle suspended in silicone oil at $\dot{\gamma} = 10$ and 100 s^{-1}.

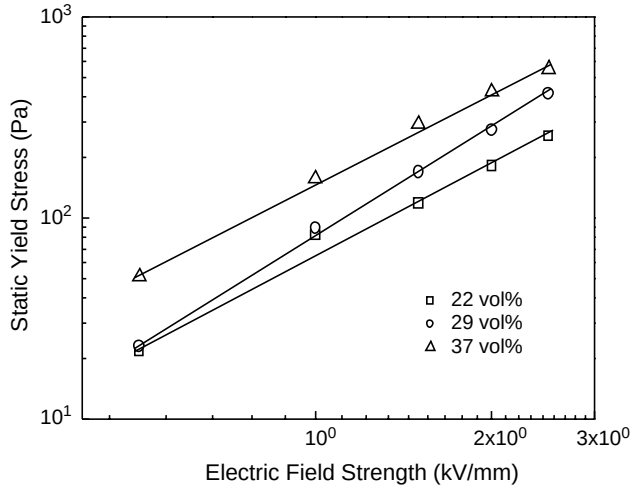

Fig. 5. Static yield stress for chitosan suspension with various concentrations (22, 29, and 37 vol%) at five different electrical field strengths.

$$\tau_y(E_0) = \kappa E_0^2 \left[\frac{\tanh\sqrt{E_0/E_c}}{\sqrt{E_0/E_c}}\right] \quad (2)$$

where κ depends on the dielectric constant and the particle volume fraction, and E_c is the critical electric field strength, which is proportional to the particle conductivity. We also found that E_c is influenced by the conductivity mismatch between the particle and medium liquid and is weakly dependent on the volume fraction. Generally, the correlation of the yield stress (τ_y) on the electric field strength (E_0) was represented by the power law model [33,34].

$$\tau_y \propto E_0^{\alpha} \quad (3)$$

The α values in this study were 1.48, 1.77, 1.48, 22, 29, and 37 vol%, respectively. These results in this study deviate from the exponent from the polarization model [35] in which yield stress is proportional to the square of electric field strength, E^2. The polarization is considered to maintain chain-like structures formed by particles dispersed in oil under an external applied electric field. Furthermore, the particle shape affected the polarization behavior. The response of ER fluid becomes nonlinear through electrical breakdown at high electric field strengths and under applied shear rate.

Fig. 6 represents the plot of dynamic yield stress (τ_{dyn}) vs. $\phi E^{1.5}$ for chitosan particles based ER fluids. The curve presents a linear fitting: $\tau_{dyn} = 312.5\phi E^{1.5}$. The, τ_{dyn}, extrapolation value of the plateau region in the flow curves given in Fig. 3, depends on the particle's attractive forces. The conductivity among the stationary adjacent particles is affected in ER response resulting from the conduction model which described a static model [36]. τ_{dyn} depends on the E range that it shows 2 until reaching the E_c and becomes smaller than 2 as $E > E_c$ [37]. The interfacial polarization is reported that the fibrillar structures are formed by particle's rotation under external electric field [38].

It is well-known that the polarization model shows a good agreement [39–41] with the data for small ϕ and E_0. However, the dynamic yield stress data deviate significantly from the

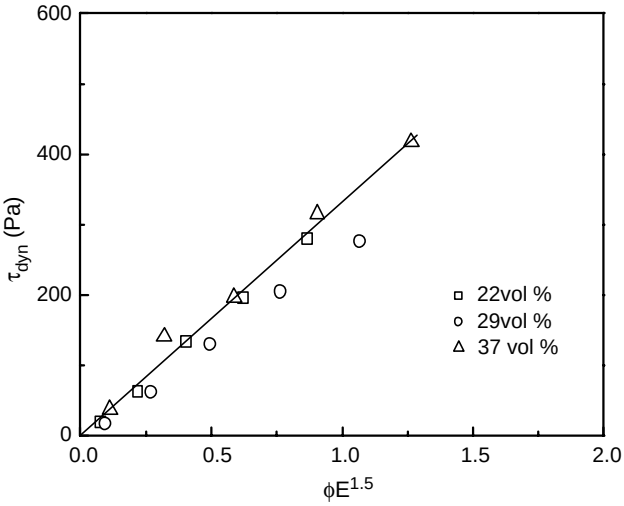

Fig. 6. τ_{dyn} vs. $\phi E^{1.5}$ for chitosan particle based ER fluids.

polarization model at high E_0 and are better represented by the power law relationship as given in Eq. (3) (α comes out to be smaller than 2). Note that $\alpha = 2$ in the polarization model, while $\alpha = 1.5$ in the conduction model.

As the gap between the conducting particles in the fluid decreases, the electric response of the fluid becomes nonlinear, e.g. electrical breakdown or particle discharge at the high electric field strength occurs. In this case, the ER effect is caused by the fluid-induced conductivity enhancement among nearly touching particles. The conductivity mismatch between particles and liquid media, rather than the dielectric constant mismatch, was considered to be a dominant factor for the Dc and low frequency Ac excitation [42]. The conduction model considers the particle interaction only and does not take into account the microstructural changes, which occurs after the application of an electric field.

In other viewpoint of the nonlinear conductivity effect considered in bulk conducting particle model and yield-stress model fitting, the power law index approaches 3/2 at high E. From this result, E_c separates the two different slopes for E_0 vs. τ_y plot [43]. Eq. (2) provides the following two limiting behaviors [44] for τ_y

$$\tau_y(E_0) = \kappa E_0^2 \left(\frac{\sqrt{E_0/E_c}}{\sqrt{E_0/E_c}}\right) \propto E_0^2$$

since

$$\tanh\sqrt{\frac{E_0}{E_c}} = \left(\frac{E_0}{E_c}\right)^{1/2} - \frac{1}{3}\left(\frac{E_0}{E_c}\right)^{3/2} + \cdots \cong \left(\frac{E_0}{E_c}\right)^{1/2} \quad (4)$$

for $E_0 << E_c$

On the other hand,

$$\tau_y(E_0) = \kappa E_0^2 \left(\sqrt{\frac{E_0}{E_c}}\right)^{-1} = \kappa\sqrt{E_c}E_0^{3/2} \propto E_0^{3/2}$$

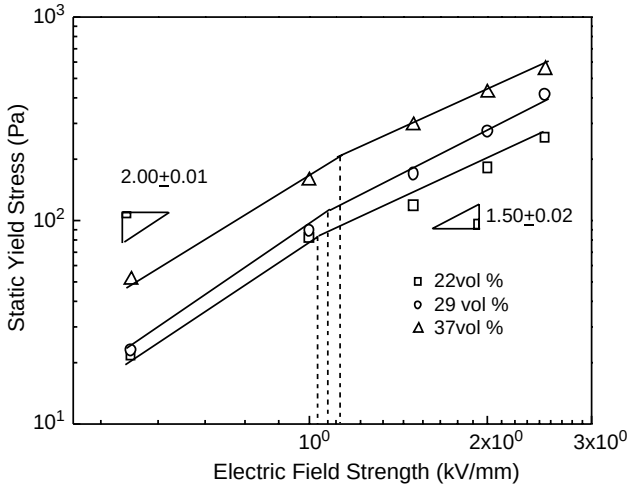

Fig. 7. Static yield stress for chitosan suspension plotted based on both polarization model and conduction model.

since

$$\tanh\sqrt{\frac{E_0}{E_c}} \cong 1 \quad \text{for } E_0 >> E_c \tag{5}$$

E_c stemmed from the nonlinear conductivity model, and represented the crossover behavior as shown in Fig. 7. E_c appears to be proportional to the particle conductivity and is influenced by the conductivity mismatch between the suspended particle and liquid media [45]. Furthermore, it can be noted that the error in the value of E_c does not influence the conclusion in the universal scaling.

We normalized Eq. (2) with E_c and $\tau_y(E_c)$ to collapse the data into a single universal curve. We could express as following:

$$\hat{\tau} = 1.313\hat{E}^{3/2}\tanh\sqrt{\hat{E}} \tag{6}$$

where $\hat{E} \equiv E_0/E_c$ and $\hat{\tau} \equiv \tau_y(E_0)/\tau_y(E_c)$ with $\tau_y(E_c) = \kappa E_c^2$ $\tanh(1) = 0.726\kappa E_c^2$. The chitosan data are found to be collapsed onto a single curve using Eq. (6), as shown in Fig. 8, fitting for three different volume concentrations. The beauty and the benefits of the employment of this universal scaling include that not only this scaling can connect the polarization and conductivity models smoothly together, but also it can predict the performance of certain ER materials with limited experimental data. It is well known that to obtain a yield stress at a relatively high applied electric field above 10 kV/mm is generally difficult due to electric current or limitation of the measuring apparatus. In addition, please note that even though our universal yield stress model is not derived from first principles, it is important for representing data by experimentalists as we mentioned it in our first report regarding this [44].

Furthermore, to examine shear rate ($\dot{\gamma}$) dependence on the shear stress (τ), we decouple τ as flow-dependent part ($\dot{\gamma}$) and flow-independent point (ϕ, E) as a functional formula of $\Phi_2(\lambda\dot{\gamma})$ and $\Phi_1(\phi, E)$, respectively [46].

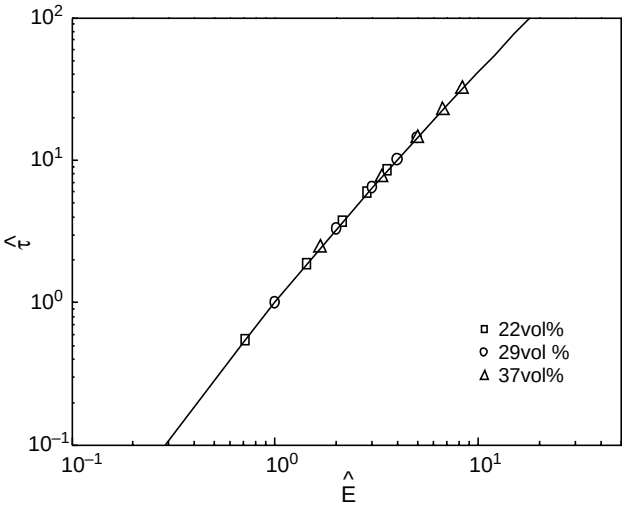

Fig. 8. The universal curve for $\hat{\tau}$ vs. $\hat{E}$ for 22, 29, and 37 vol% chitosan particles in silicone oil.

$$\tau(\dot{\gamma}, \phi, E) = \Phi_1(\phi, E)\Phi_2(\lambda\dot{\gamma}) \tag{7}$$

$$\frac{\tau(\dot{\gamma}, \phi, E)}{\Phi_1(\phi, E)} = \Phi_2(\lambda\dot{\gamma})$$

Here, λ is related to the dielectric constant of materials in ER suspension and

$$\lambda = \frac{16\eta_c}{\varepsilon_0\varepsilon_c\delta^2E^2} \tag{8}$$

where, η_c (viscosity of the suspension medium) = 0.048 (Pa s), ε_0 (permittivity of free space) = 8.8542×10^{-12} (F m^{-1}), ε_c (dielectric constant of the silicone oil at 100 Hz) [47] = 2.5 ε_0, ε_p (dielectric constant of chitosan particles at 100 Hz) = 11.77 ε_0, and $\delta = (\varepsilon_p - \varepsilon_0)/(\varepsilon_p + 2\varepsilon_c) = 0.77$ [48]. Fig. 9 represents the universal curves for τ/Φ_1 (ϕ, E) vs. $\lambda\dot{\gamma}$ at three different particle concentrations through Eqs. (7) and (8). The flow curves are approximately in a single line with some fluctuations due to its slight departure of E^2 dependence on yield stress.

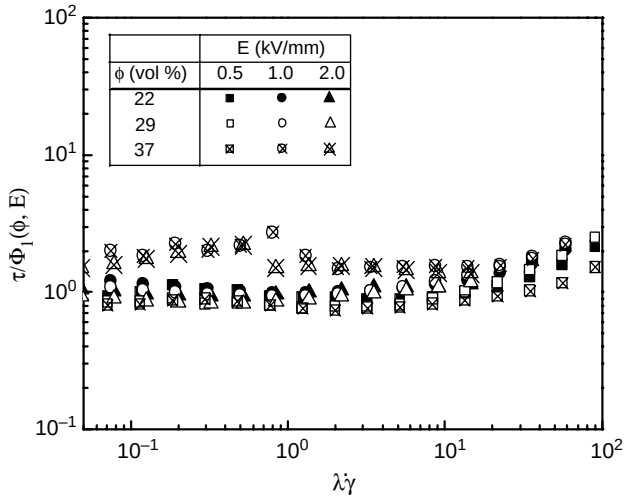

Fig. 9. Universal flow curve for chitosan based ER fluids for three different particle concentrations and electric field strengths.

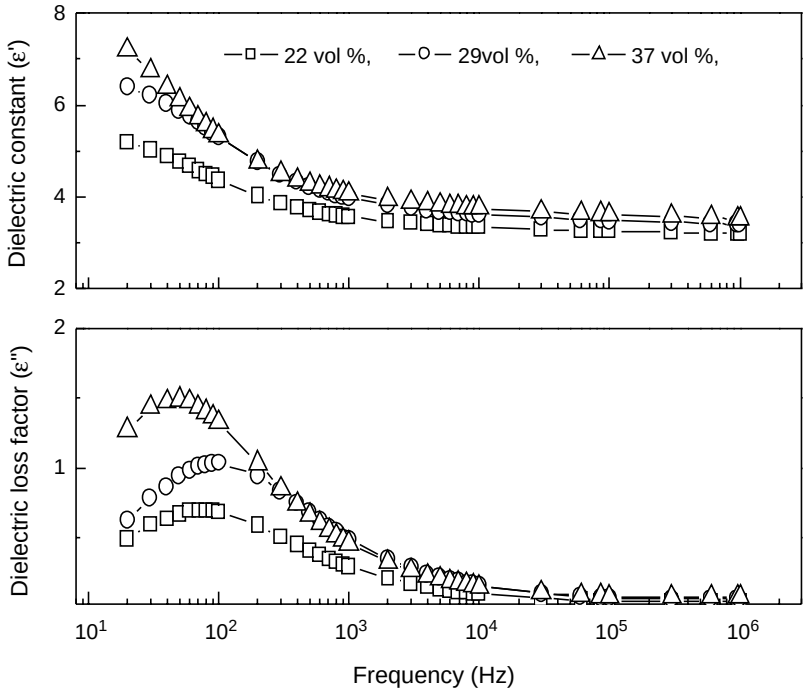

Fig. 10. Dielectric spectra for three different concentrations (22, 29, and 37 vol%) of chitosan suspension.

Since the magnitude of the dielectric constant is related to the molecular structure, its dependence on time, frequency, and temperature generally reflects molecular motion. Fig. 10 shows dielectric relaxation spectra of the suspended chitosan in silicone oil. The characteristics of interfacial polarization are represented by dielectric constant (ε') and dielectric loss factor (ε'') [49,50], and fitted with the Cole–Cole formula [51] of dielectric relaxation data.

$$\varepsilon^* = \varepsilon' + \mathrm{i}\varepsilon'' = \varepsilon'_\infty + \frac{\varepsilon'_0 - \varepsilon'_\infty}{1 + (\mathrm{i}\omega\lambda_\varepsilon)^{1-\alpha}} \quad (0 \le \alpha < 1) \tag{9}$$

where $\varepsilon'_0 = \lim_{\omega\to 0} \varepsilon^*(\omega)$ and $\varepsilon''_0 = \lim_{\omega\to\infty} \varepsilon^*(\omega)$. λ_ε is the relaxation time for the interfacial polarization, which is estimated from the following Eq. (11). The relaxation frequency at which the ε'' had a local maximum is very important for electrorheology due to the rate of polarization of particles. If $\alpha = 0$, Eq. (9) represents Debye model which has a single relaxation time. By fitting the Cole–Cole plot (Fig. 11), the value of ε'_0 was estimated to be 5.8, 7.3, and 9.1 for chitosan particles at the concentrations of 22, 29, and 37 vol% in silicone oil, respectively as summarized in Table 1. Among the parameters in the Cole–Cole plot, the relaxation time of interfacial polarization (λ_ε) and an achievable polarizability ($\Delta\varepsilon = \varepsilon_0 - \varepsilon_\infty$) are related with the yield stress and stress enhancement under an applied electric field [52].

Table 1
Parameters in Eq. (9) for chitosan based ER fluid with three different concentrations

Chitosan concentration (vol%)	ε_0	ε_∞	$\Delta\varepsilon = \varepsilon_0$-$\varepsilon_\infty$	λ (ms)	α
22	5.8	3.36	2.24	2.3	0.26
29	7.3	3.62	3.68	1.6	0.28
37	9.1	3.84	5.26	3.2	0.28

The λ reflects the rate of interfacial polarization when an external electric field is applied, so that it is mainly related to the stress increase during deformation under a shear field, and $\Delta\varepsilon$ shows the degree of polarization, which is related to the electrostatic interaction between particles. As the concentration of chitosan increases, $\Delta\varepsilon$ increases. Polarization consists of interfacial, dipole-orientation, as well as ionic and electronic polarizations. The polarization rate is inversely proportional to the relaxation frequency.

$$\lambda_\varepsilon = \frac{1}{2\pi f_c} \tag{10}$$

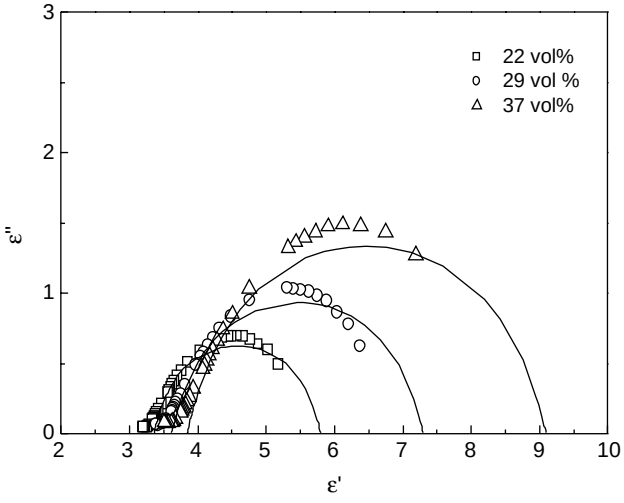

Fig. 11. Cole–Cole plot of for three different concentrations (22, 29, and 37 vol%) of chitosan suspension.

The frequency, f_c corresponds to the maximum value for ε'' or for which ε' represents the steepest descent with frequency [51]. The connection between dielectric measurements made in the frequency and time domain are related by the Fourier transform relation. The ε'' vs. frequency of the chitosan based ER fluids showed the maximum frequency in Fig. 10. We obtained the relaxation time from the Eq. (10) for each system: 70 Hz for 22 vol%, 100 Hz for 29 vol%, and 50 Hz for 37 vol%. The relaxation time is calculated to be 2.3 ms for 22 vol%, 1.6 ms for 29 vol%, and 3.2 ms for 37 vol%, respectively .

The λ and $\Delta\varepsilon$ obtaining from the dielectric spectrum of ER fluid are demonstrated by resulting in the difference of the flow behavior and ER performance. Although the λ shows the higher value in chitosan 29 vol% than that of other ER fluids, the highest $\Delta\varepsilon$ of chitosan based ER fluid shows in the higher particular concentration (in case of 37 vol%) meaning the strongest particular attraction among ER fluids. Therefore, it can be considered that $\Delta\varepsilon$ value is more effective and dominant for ER performance because it is directly related to the strength of particulate fibril structures [53–56].

4. Conclusions

A chitosan suspension in silicone oil showed the ER response upon the application of the electric field and this suspension behaved as a Bingham fluid. ER property of chitosan suspension was determined by the polarizability of the branched amino polar group of the chitosan particles, whose micro-structural properties changes during flow. These systems were correlated well with the universal scaling curve for the yield stress at the given critical electric field strength. We also investigated flow-dependent scaling analysis by constructing a dimensionless group for shear rate. The chitosan based ER fluid was also examined from the electrical relaxation analysis obtained from the dielectric spectrum.

Acknowledgements

This work was supported by research grants from the Korea Science and Engineering Foundation (KOSEF) through the Applied Rheology Center (ARC).

References

[1] Tao R, Sun JM. Phys Rev Lett 1991;67:398–401.
[2] Trlica J, Sáha P, Quadrat O, Stejskal J. Physica A 2000;283:337–48.
[3] Ma H, Wen W, Tam WY, Sheng P. Adv Phys 2003;52:343–83.
[4] Lim ST, Cho MS, Choi HJ, Jhon MS. J Ind Eng Chem 2003;9:336–9.
[5] Jang IB, Kim HB, Lee JY, You JL, Choi HJ, Jhon MS. J Appl Phys 2005; 97:10Q912.
[6] Kim SG, Kim JW, Cho MS, Choi HJ, Jhon MS. J Appl Polym Sci 2001; 79:108–14.
[7] Choi HJ, Kim JW, To K. Polymer 1999;40:2163–6.
[8] Woo DJ, Suh MH, Shin ES, Lee CW, Lee SH. J Colloid Interface Sci 2005;288:71–4.
[9] Lengalova A, Pavlinek V, Saha P, Stejskal J, Kitano T, Quadrat O. Phyica A 2003;321:411–24.
[10] Lengalova A, Pavlinek V, Saha P, Stejskal J, Quadrat O. J Colloid Interface Sci 2003;258:174–8.
[11] Chotpattananont D, Sirivat A, Jamieson AM. Colloid Polym Sci 2004; 282:357–65.
[12] Choi HJ, Cho MS, Jhon MS. Int J Mod Phys B 1999;13:1901–7.
[13] Sim IS, Kim JW, Choi HJ, Kim CA, Jhon MS. Chem Mater 2001;13: 1243–7.
[14] Yoshimoto S. Macromol Rapid Commun 2005;26:857–61.
[15] Kim JW, Liu F, Choi HJ, Hong SH, Joo J. Polymer 2003;44:289–93.
[16] Choi HJ, Kim JW, Cho MS, Kim CA, Jhon MS. Int J Mod Phys 2002;16: 2636–42.
[17] Choi US, Park YS. J Ind Eng Chem 2001;7:281–4.
[18] Wu S, Shen J. J Appl Polym Sci 1996;60:2159–64.
[19] Wu S, Zeng F, Shen J. J Appl Polym Sci 1998;67:2077–82.
[20] Zhao XP, Duan X. J Colloid Interface Sci 2002;251:376–80.
[21] Hirano SI, Yogo T, Sakamoto W, Banno K, Fukuzawa R. J Eur Ceramic Soc 2004;24:1911–7.
[22] Ogawa K, Yui T. Biosci Biotech Biochem 1993;57:1466–9.
[23] Golomb G, Levi M, Gelder JMV. J Appl Biomater 1992;3:23.
[24] Chandy T, Sharma CP. Biomaterials 1992;13:949–52.
[25] Sung JH, Choi HJ, Sohn JI, Jhon MS. Colliod Polym Sci 2003;281: 1196–200.
[26] Jang WH, Cho YH, Kim JW, Choi HJ, Shon JI, Jhon MS. J Mater Sci Lett 2001;20:1029–31.
[27] Park SJ, Cho MS, Lim ST, Choi HJ, Jhon MS. Macromol Rapid Commun 2005;26:1563–6.
[28] Choi HJ, Lee JH, Cho MS, Jhon MS. Polym Eng Sci 1999;39:493–9.
[29] Kim SG, Choi HJ, Jhon MS. Macromol Chem Phys 2001;202:521–6.
[30] Halsey TC. Phys Rev Lett 1992;68:1519–22.
[31] Yin JB, Zhao XP. Chem Mater 2002;14:4633–40.
[32] Conrad H, Wu C, Tang X. Int J Mod Phys B 1999;13:1729–38.
[33] Block H, Kelly JP. J Phys D: Appl Phys 1988;21:1661–7.
[34] Klass DL, Martinek TW. J Appl Phys 1967;38:67–74.
[35] Klingenberg DJ, Swol F, Zukoski CF. J Chem Phys 1991;94:6170–8.
[36] Wu C, Chen Y, Conrad H. J Phys D: Appl Phys 1998;31:960–3.
[37] Ikazaki F, Kawai A, Uchida K, Kawakami T, Edmura K, Sakurai K, et al. J Phys D: Appl Phys 1998;31:336–47.
[38] Hao T, Kawai A, Ikazaki F. Langmuir 1998;14:1256–62.
[39] See H. J Ind Eng Chem 2004;10:1132–45.
[40] Duan X, Chen H, He Y, Luo W. J Phys D: Appl Phys 2000;13:696–9.
[41] Klingenberg DJ, Zukoski CF. Langmuir 1990;6:15–24.
[42] Davis DC. J Appl Phys 1992;72:1334–40.
[43] Davis LC. J Appl Phys 1997;81:1985–91.
[44] Choi HJ, Cho MS, Kim JW, Kim CA, Jhon MS. Appl Phys Lett 2001;78: 3806–8.
[45] Sung JH, Hong CH, Park BJ, Choi HJ, Jhon MS. Scripta Mater 2005;53: 1101–3.
[46] Ghosh P, Siddhanta SK, Chakrabarti A. Eur Polym J 1997;35:699–710.
[47] Bodek KH, Bak GW. Eur J Pharm Biopharm 1999;48:141–8.
[48] Mitsumata T, Sugitani K. Macromol Rapid Commun 2004;25:848–52.
[49] Lengalova A, Pavlinek V, Saha P, Quadrat O, Stejskal J. Colloid Surf A 2003;227:1–3.
[50] See H, Kawai A, Ikazaki F. Colloid Polym Sci 2002;280:24–9.
[51] Block H, Kelly JP, Qin A, Watson T. Langmuir 1990;6:6–14.
[52] Cho MS, Cho YH, Choi HJ, Jhon MS. Langmuir 2003;19:5875–81.
[53] Cho MS, Choi HJ, Ahn WS. Langmuir 2004;20:202–7.
[54] Sung JH, Cho MS, Choi HJ, Jhon MS. J Ind Eng Chem 2004;10:1217–29.
[55] Wang BX, Zhao XP. J Mater Chem 2002;12:2869–71.
[56] Park BJ, Sung JH, Lee IS, Choi HJ. Chem Phys Lett 2005;414:525–6.